Brain and Spine 5 (2025) 104187

Contents lists available at ScienceDirect

Brain and Spine

journal homepage: www.journals.elsevier.com/brain-and-spine

Intraoperative classification of CNS lymphoma and glioblastoma by AI-based analysis of Stimulated Raman Histology (SRH)

Pierre Scheffler [a,b], Jakob Straehle [a,b], Amir El Rahal [a,b], Daniel Erny [c], Boris Mizaikoff [b,d], Ioannis Vasilikos [a,b,e], Marco Prinz [b,c], Volker A. Coenen [b,f], Julia Kühn [e,g], Florian Scherer [g,h], Dieter Henrik Heiland [a,b,h,i], Oliver Schnell [a,b,i], Roland Roelz [a,b], Jürgen Beck [a,b], Peter C. Reinacher [f,j], Nicolas Neidert [a,b,e,h,*]

[a] Department of Neurosurgery, Medical Center, University of Freiburg, Freiburg, Germany
[b] Center for Advanced Surgical Tissue Analysis (CAST), Faculty of Medicine, University of Freiburg, Freiburg, Germany
[c] Institute of Neuropathology, Faculty of Medicine, University of Freiburg, Freiburg, Germany
[d] Institute of Analytical and Bioanalytical Chemistry, Ulm University, Ulm, Germany
[e] Berta-Ottenstein Programme, Faculty of Medicine, University of Freiburg, Germany
[f] Department of Stereotactic and Functional Neurosurgery, Medical Center, University of Freiburg, Freiburg, Germany
[g] Department of Medicine I, Medical Center—University of Freiburg, Faculty of Medicine, University of Freiburg, Freiburg, Germany
[h] German Cancer Consortium (DKTK), partner site Freiburg, Germany
[i] Department of Neurosurgery, Medical Center, Faculty of Medicine, Erlangen University, Erlangen, Germany
[j] Fraunhofer Institute for Laser Technology (ILT), Aachen, Germany

ARTICLE INFO

Handling editor: Dr W Peul

Keywords:
Stimulated Raman histology
CNS lymphoma
Glioblastoma
Machine learning

ABSTRACT

Introduction: Early diagnosis is important to differentiate central nervous system lymphomas (CNSL) from the main differential diagnosis, glioblastoma (GBM), because of different primary treatment modalities for these entities. Due to neurological deficits, diagnostic stereotactic biopsies often need to be performed urgently. In this setting the availability of an intraoperative neuropathological assessment is limited.
Research question: This study uses AI-based analysis of Stimulated Raman Histology (SRH) to establish a classifier distinguishing CNSL from glioblastoma in an intraoperative setting.
Material and methods: We collected 126 intraoperative SRH images from 40 patients diagnosed with CNSL. These SRH images were divided into patches, measuring 224 x 224 pixels each. Additionally, we used a comparative dataset of 87 SRH images from 31 patients with GBM as a control group to train and validate a neural network based on the CTransPath architecture. Two distinct diagnostic categories were established: “Lymphoma” and “Glioblastoma".
Results: Our model demonstrated an accuracy rate of 92.5% in distinguishing between lymphoma and glioblastoma. Analysis of our test dataset showed a sensitivity of 84.2% and a specificity of 100% in the detection of CNSL, demonstrating performance comparable to standard intraoperative histopathological analysis.
Discussion and conclusion: The use of AI-driven analysis of SRH images holds promise for intraoperative tissue examination of stereotactic biopsies with suspected CNSL en par with the current gold standard. This study could improve the management of these cases especially in the emergency setting when conventional intraoperative neuropathological evaluation is unavailable.

1. Introduction

Central nervous system lymphoma (CNSL) is a rare type of primary brain tumor, accounting for approximately 2–5% of all brain lesions (Lukas et al., 2018). Most of these cases are primary CNSL, with no manifestation outside the brain or spinal cord histologically classified as diffuse large cell B-cell lymphoma (DLBCL). In contrast to other CNS malignancies, first-line therapy is methotrexate-based immunochemotherapy (Schorb et al., 2016). Primarily resection is not indicated (Hoang-Xuan, 2023).

* Corresponding author. Department of Neurosurgery, Medical Center, University of Freiburg, Freiburg, Germany.
E-mail address: nicolas.neidert@uniklinik-freiburg.de (N. Neidert).

https://doi.org/10.1016/j.bas.2025.104187
Received 15 September 2024; Accepted 13 January 2025
Available online 26 January 2025

As a result, early identification of CNSL is crucial for adequate management. Modern MRI techniques and MR-based classifiers are advancing but are not yet sufficient to reliably differentiate CNS lymphomas from other tumor entities, especially glioblastomas (GBM)(Du et al., 2022). Both tumors show contrast enhancement in T1 MRI after application of a gadolinium-based agent, and both are usually intra-axial lesions. To this date, stereotactic brain biopsy plays a key role in the definitive diagnosis of CNSL.

Patients with lesions suspicious for CNSL often present with rapidly progressing neurological symptoms. These symptoms can be improved with administration of corticosteroids. Corticosteroids reduce the perifocal edema in most brain tumors. In CNSL, it also leads to a significant reduction of tumor size (Scheichel et al., 2021). Unfortunately, this also leads to a reduced diagnostic accuracy of stereotactic brain biopsies in CNSL (Scheichel et al., 2021). Consequently, brain biopsy should be performed before administration of corticosteroids if possible. To relieve neurological symptoms by corticosteroid treatment, brain biopsies in suspected CNSL are therefore performed in an emergency setting. However, emergency histopathological analyses are usually unavailable in this setting, even in many large medical centers. As a result, technologies that enable rapid and automated histopathological imaging and analysis would be highly useful in such cases.

Stimulated Raman Histology (SRH) microscopy is a novel histopathological imaging technique that provides label-free chemical contrast within minutes (Orringer et al., 2017; Hollon and Orringer, 2021). SRH is based on Stimulated Raman Scattering (SRS)(Freudiger et al., 2008), which can be used for intraoperative histopathological diagnostic imaging of comparable quality to H&E sections (Straehle et al., 2022; Eichberg et al., 2019; Hollon et al., 2020). As SRS microscopy creates digital SRH images in a consistent and reproducible manner, SRS histopathological images represent an excellent dataset for training of neural networks. Previous publications have shown that SRS microscopy can even be used to reliably predict features such as isocitrate dehydrogenase (IDH)-mutations, 1p19q-codeletions and loss of ATP-dependent helicase (ATRX) in gliomas (Hollon et al., 2023).

In this study, we describe the training of a combined convolutional neural network and vision transformer with SRH images obtained from stereotactic brain biopsies of GBM and CNSL tumors. Model performance was assessed in an independent test dataset of SRH-images.

2. Methods

2.1. Sample collection

Tissue samples were obtained intraoperatively from frame-based stereotactic brain biopsies of patients with suspected CNSL (Fig. 1A) except in 2 CNSL cases, where microsurgical resection was performed due to presumed GBM. All biopsies were taken for diagnostic purposes. Prior to surgery, all patients or their designated caregivers provided informed written consent for sample collection and subsequent analysis. The study was approved by the local ethics committee (ethical approval number: 23-1175-S1) and it was carried out in accordance to the Declaration of Helsinki.

Tissue was mounted on an object holder and imaged using the NIO Laser Imaging System with standard settings (Invenio Imaging Inc., Santa Clara, CA, USA). Several regions of interest with varying sizes ranging from 0.8 mm × 0.9 mm–6.7 mm × 7.4 mm were imaged and saved for further processing (Neidert et al., 2022).

2.2. Image preprocessing

Raw 16-bit grayscale images from the CH2 and CH3 channel (2845 cm^{-1} and 2940 cm^{-1}) were converted to 8-bit RGB H&E-like images by recoloring using a lookup table provided by the manufacturer. A total of 250 patches with a size of 224 by 224 pixels each were extracted from each original image at random locations for further processing by the neural network (Fig. 1B).

2.3. Machine learning and model training

We based our machine learning model on the CTransPath architecture (Wang et al., 2022). CTransPath is a hybrid architecture that integrates a convolutional neural network and a transformer architecture. Both architectures have previously been successfully applied to image processing and represent the current state of the art for image classification (Le et al., 2021). CTransPath has been pretrained on a large

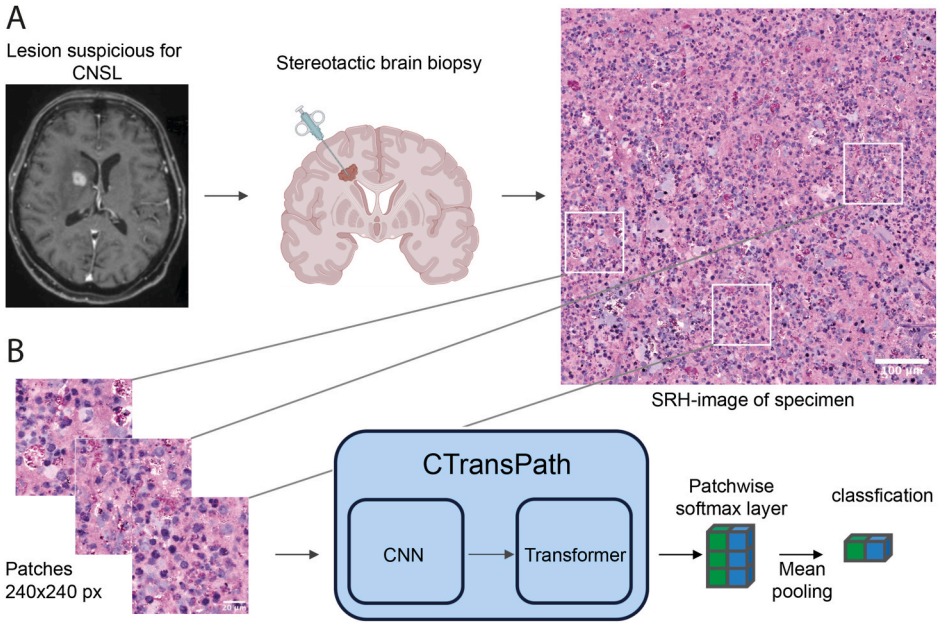

Fig. 1. (A) Patients with cerebral lesions suspicious for CNSL are included in this study. SRH-images were obtained using tissue from stereotactic biopsies intraoperatively. In A, an example of a SRH-image of a CNSL is shown. (B) The SRH-images of 80% of the patients were used for training and validation of our model. The SRH-images of 20% of the patients were reserved for the test dataset. 250 randomly selected patches of 224x224 pixels per image were used to train the CTransPath architecture.

dataset of unlabeled histopathological images for the purpose of feature extraction, which allows to finetune the model on a significantly smaller dataset (Wang et al., 2022).

The complete data set was divided into a test dataset and a validation and a training dataset. A total of 20% of patients were randomly allocated to the test dataset. SRH images from the remaining patients were used for training and validation, in a 4:1 ratio.

The model was trained based on image patches extracted from SRH images, with the histopathological diagnosis (lymphoma or glioblastoma) serving as the label. The training process was conducted for a total of 10 epochs, utilizing stochastic gradient descent as the optimization algorithm and cross-entropy as the loss function. The model exhibiting the lowest validation loss was selected for prediction.

2.4. Model testing

The assessment of the model's performance was conducted using the test dataset. For this evaluation, individual predictions (based on the softmax layer) for the patches extracted from each image were aggregated using mean pooling (Fig. 1B), resulting in a classification of each image as either lymphoma or glioblastoma. The code is publicly available under github.com/pierreschеffler/srh_lymphoma.

3. Results

3.1. Patient population

In total, 213 SRH images from 40 patients with a definitive histopathological diagnosis of CNSL and 31 patients with glioblastoma were subjected to analysis (see Table 1). All cases of CNSL were classified as DLBCL in the subsequent histopathological workup. A total of 75% (30/40 patients) of lymphomas were identified as primary CNSL, while 25% of cases were classified as secondary CNSL.

The median age of patients with CNSL was similar to that of glioblastoma patients (69.52 vs 68.42 years). In patients diagnosed with CNSL stereotactic biopsies were more frequently performed in an emergency setting in comparison to patients with glioblastoma. In total, 29.58% of the biopsies were conducted in an emergency setting without the availability of conventional intraoperative neuropathological assessment.

3.2. Model performance

Of the total 213 images, 173 were included in the training dataset, 66 derived from GBM patients and 107 from CNSL patients. Model performance was assessed on image-level using a total of 40 SRH-images from the test dataset. This dataset comprises 21 images derived from GBM samples, and 19 images derived from CNSL samples. SRH-images of the tumor from the same patients were not included in both datasets. The model showed an F1-score of 0.9143 with a threshold of 0.9 for prediction of an SRH-image as CNSL (Fig. 2A). In order to optimize for specificity, the cutoff for further analysis was set to 0.9. The receiver operating characteristic (ROC) curve analysis for this model demonstrates an area under the curve (AUC) of 0.972 (Fig. 2B).

The mean pooling of the softmax layer for the analyzed patches of one image was employed to predict the probability of classification as CNSL. The aggregate probability of either "Lymphoma" or "Glioblastoma" for each image is represented in a box plot for each SRH-image in the test dataset (Fig. 3A). Using the defined threshold of 0.9 on the test dataset, 16 of 19 lymphoma images were correctly classified as lymphoma. Three images were misclassified as glioblastoma. All 21 images of glioblastoma were correctly classified as glioblastoma. This results in a specificity of 100% and a sensitivity of 84.2% for the prediction of CNSL. The results are visualized in a confusion matrix (Fig. 3B). The overall accuracy of the model is 92.5%.

Table 1
Patient characteristics of the cohort. The patients'age ranged in the CNSL group from 45 to 84 years and in the GBM group from 29 to 92 years.

	CNS-Lymphoma	Glioblastoma
Number of patients	40	31
Number of SRH-images	126	87
Mean Age (years)	69.65	68.42
Sex (m:f)	18:22	16:15
Emergency Biopsy	37.5%	19.35%

3.3. Visualization of model predictions

In order to facilitate the interpretation of the model's output and identify relevant image-areas for classification as lymphoma or glioblastoma, heatmaps of the predictions of lymphoma and glioblastoma images over the original images were plotted. For illustrative purposes, examples are provided in Fig. 4. A comparison of the heatmaps with the original SRH images reveals that areas exhibiting dense tumor infiltration are highlighted. This indicates that the tumor cells are being identified in a manner that is distinct from the recognition of surrogate parameters such as preparation artefacts or tissue reactions.

4. Discussion

This study presents an artificial intelligence (AI)-based analysis tool for intraoperative Stimulated Raman Histology (SRH) imaging, capable of differentiating between CNSL and GBM samples. The tool demonstrated performance in a test dataset, with a sensitivity of 84%, a specificity of 100% and an overall accuracy of 925%.

Intraoperative crush cytology or frozen section analysis are the current gold standard methods for rapid intraoperative tumor differentiation in stereotactic biopsies (Kahraman et al., 2024). As it requires both experience in sample preparation and histological interpretation it is not always a readily available option. SRH imaging particularly with automated analysis represents a straightforward and accessible technique. Therefore, intraoperative SRH is increasingly used for many different applications. The application of AI-based analysis to SRH has demonstrated the capacity to differentiate between tumor and non-tumor lesions (Pekmezci et al., 2021), to distinguish between different brain tumor entities (Hollon et al., 2020) and can even detect molecular genetic features in glioma (Hollon et al., 2023). SRH-images are ideal substrates for machine learning as batch effects for sample preparation, tissue staining, imaging and processing of data are reduced to a minimum. Multicenter pooling of SRH-images can increase model performance as investigator biases are very limited (Reinecke et al., 2024).

Other tools that have been designed for the purpose of identifying CNSL are based on Raman spectroscopy, as demonstrated by Klamminger et al. (2021). Like SRH, Raman spectroscopy can be employed for rapid intraoperative tumor analysis. However, spectroscopy does not permit for spatial contextualization and actual histological imaging, resulting in classification performance that is inferior to both regular intraoperative histology and SRH with an diagnostic accuracy of only 82.4% (Klamminger et al., 2021).

Concerning our results, we have demonstrated a diagnostic accuracy that is comparable to the current standard for intraoperative histology. Reported accuracies in the literature from classical rapid intraoperative diagnosis for the diagnosis of CNS lymphoma from crush cytology or frozen sections range from 72% to 89.6% (Kahraman et al., 2024; Sugita et al., 2014). Even after using time-intensive immunohistochemistry for these cases, classical neuropathological assessment reaches an accuracy of 92.3% (Morell et al., 2019). However, our approach offers the advantage of automated histological analysis, which does not require intervention by a pathologist. As a result, SRH analysis can be conducted in emergency settings faciliating rapid diagnosis. Nevertheless, the

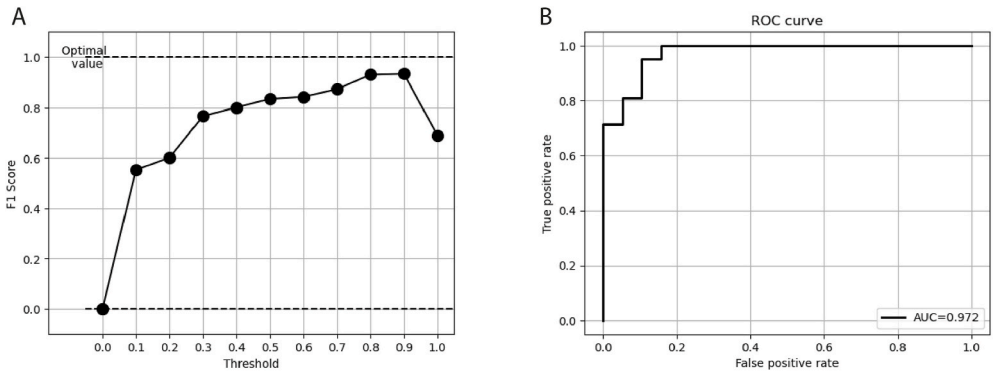

Fig. 2. (A) The F1-score is plotted for different thresholds of the model for the classification of images as CNS lymphoma: The highest F1-score was achieved with a threshold of 0.9. (B) The good overall model performance is indicated by the shown ROC curve resulting in an AUC of 0.972.

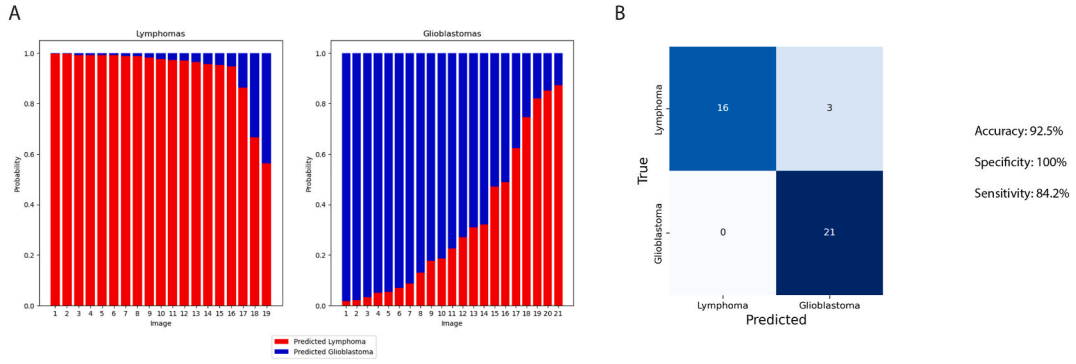

Fig. 3. (A) Mean probabilities from the softmax layer of every patch were aggregated and plotted for every image of the test-dataset. 19 images of CNS-lymphomas and 21 images of glioblastomas were evaluated. (B) Cofusion matrix showing the test results, as well as accuracy, specificity and sensitivity.

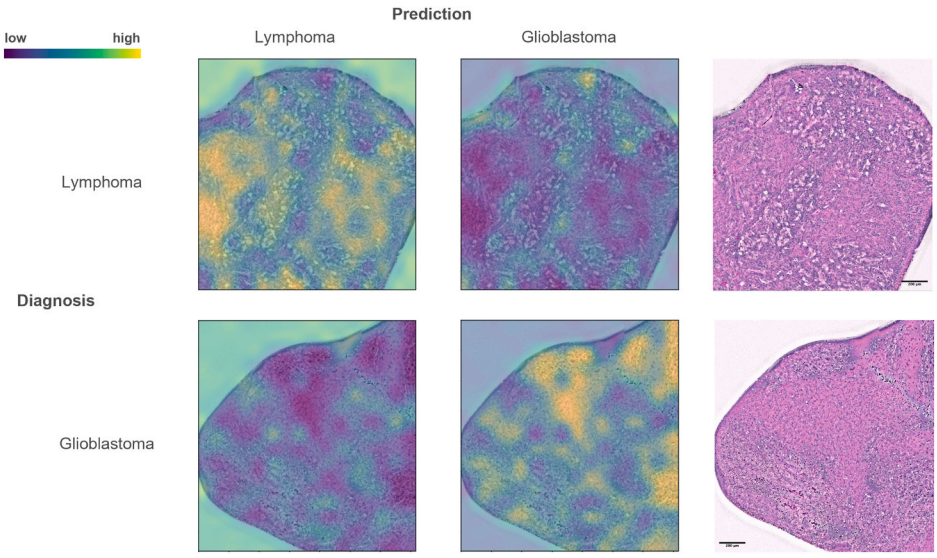

Fig. 4. 2 SRH-images of a glioblastoma and a CNS-lymphoma sample were shown in a confusion matrix. Image areas were color-coded based on the per-patch prediction of the model (blue: low probability, yellow: high probability). On the right side, the SRH-images were shown with a scale bar of 200 μm.

clinical experience and ability to contextualize information make neuropathologists indispensable for both intraoperative and final diagnoses. The classifier introduced here may prove a useful tool in assisting with intraoperative neuropathological assessment.

Intraoperative diagnosis of CNS lymphoma or glioblastoma would not alter surgical decision-making in the context of stereotactic biopsy. However, an early and accurate differentiation would inform the subsequent diagnostic pathway to start a definitive treatment as early as possible. This is particularly important in CNS lymphoma as a delay in immunochemotherapy could worsen the outcome (Rubenstein et al., 2013; Cerqua et al., 2016).

In case of a cerebral mass effect caused by a resectable tumor with inconclusive MRI, microsurgical resection of the lesion might be indicated (Hoang-Xuan, 2023; Ferreri et al., 2024). In such cases, it is of the

utmost importance to be able to differentiate between these entities intraoperatively, as this will inform the surgical decision-making process. To achieve the best possible oncological outcome, complete resection of the contrast enhancing lesion if safely feasible is the current guideline therapy. Nevertheless, this carries an increased risk of neurological deficit. In the case of a CNS lymphoma, tumor debulking would be an oncologically sufficient procedure and would not compromise the patient's neurological integrity.

A threshold of 0.9 was selected for the probability of classifying a lymphoma due to two key reasons: The threshold of 0.9 demonstrated the highest F1-value (Fig. 2A). Furthermore, a high cut-off for the classification of CNS lymphoma results in a high specificity, which is clinically relevant. A misclassification as CNS lymphoma could result in initiation of lymphoma treatment with immunochemotherapy or a potential stop of a microsurgical resection which could have adverse effects on the patient. Applying the threshold of 0.9 to the independent test cohort, we obtained a specificity of 100%.

The CTransPath-architecture was chosen as a suitable classifier for our study, because it was specifically created and trained for feature extraction in histopathological images. The averaging of predictions across patches of a larger SRH image was proved to be an effective strategy for the prediction of the histopathological diagnosis. However, larger and elaborate model architectures and more sophisticated aggregation methods could potentially enhance the accuracy of the approach.

The major limitations of our study are that it is monocentric and retrospective. Prospective and external validation of our classifier is therefore needed. In addition, intraoperative SRH has only recently become available, with only a limited number of neurosurgical departments currently equipped to perform SRH imaging.

5. Conclusion

This study demonstrates that AI-based differentiation of CNS-lymphoma and glioblastoma using Stimulated Raman Histology (SRH) achieves results comparable to conventional intraoperative histopathology. The findings suggest that AI-assisted SRH can serve as a rapid, reliable, and non-destructive alternative to traditional histopathology during neurosurgical procedures. This approach offers the potential for real-time, intraoperative decision-making, reducing the time needed for diagnosis and potentially improving surgical outcomes. Future research should focus on expanding the dataset and validating the AI model across multiple clinical settings to further confirm its effectiveness and robustness in diverse patient populations.

Disclosures

JS, RR and NN serve on an adivisory board for Servier. PCR receives research support from Else-Kroener-Fresenius Foundation, Fraunhofer Society and received personal honoraria for lectures from Arcana and is a consultant for Boston Scientific, Inomed and Brainlab. FS receives research support from Roche Sequencing Solutions, Gilead, Takeda and honoria from Servier and AstraZeneca. NN is a consultant for B.Braun. JK, IV and NN are supported by the Berta-Ottenstein Programm Förderlinie Clinician Scientist of the University Medical Center Freiburg, Germany.

Declaration of competing interests

The authors declare the following financial interests/personal relationships which may be considered as potential competing interests: Nicolas Neidert, Roland Roelz, Jakob Straehle reports a relationship with Servier Monde that includes: consulting or advisory. Peter C. Reinacher reports a relationship with Else Kröner-Fresenius Foundation that includes: funding grants. Peter C. Reinacher reports a relationship with Fraunhofer Institute for Laser Technology ILT that includes: funding grants. Peter C. Reinacher reports a relationship with Arcana Institute that includes: speaking and lecture fees. Peter C. Reinacher reports a relationship with Boston Scientific Corporation that includes: consulting or advisory. Peter C. Reinacher reports a relationship with Brainlab Inc that includes: consulting or advisory. Peter C. Reinacher reports a relationship with inomed Medizintechnik GmbH that includes: consulting or advisory. Florian Scherer reports a relationship with Roche Sequencing Solutions Inc that includes: funding grants. Florian Scherer reports a relationship with Gilead Sciences Inc that includes: funding grants. Florian Scherer reports a relationship with Takeda Oncology that includes: funding grants. Florian Scherer reports a relationship with AstraZeneca Pharmaceuticals LP that includes: speaking and lecture fees. Florian Scherer reports a relationship with Servier that includes: speaking and lecture fees. Nicolas Neidert reports a relationship with B Braun SE that includes: consulting or advisory. JK, IV and NN are supported by the Berta-Ottenstein Programm Förderlinie Clinician Scientist of the University Medical Center Freiburg, Germany. If there are other authors, they declare that they have no known competing financial interests or personal relationships that could have appeared to influence the work reported in this paper.

Acknowledgements

We thank B. Baumer, O. Mueller and V. Sacalean for their excellent technical support.

References

Cerqua, R., et al., 2016. Diagnostic delay and prognosis in primary central nervous system lymphoma compared with glioblastoma multiforme. Neurol. Sci. 37, 23–29.
Du, X., He, Y., Lin, W., 2022. Diagnostic accuracy of the diffusion-weighted imaging method used in association with the apparent diffusion coefficient for differentiating between primary central nervous system lymphoma and high-grade glioma: systematic review and meta-analysis. Front. Neurol. 13, 882334.
Eichberg, D.G., et al., 2019. Stimulated Raman histology for rapid and accurate intraoperative diagnosis of CNS tumors: prospective blinded study. J. Neurosurg. 1–7. https://doi.org/10.3171/2019.9.JNS192075.
Ferreri, A.J.M., et al., 2024. Primary central nervous system lymphomas: EHA-ESMO Clinical Practice Guideline for diagnosis, treatment and follow-up. Hemasphere 8, e89.
Freudiger, C.W., et al., 2008. Label-free biomedical imaging with high sensitivity by stimulated Raman scattering microscopy. Science 322, 1857–1861.
Hollon, T., Orringer, D.A., 2021. Label-free brain tumor imaging using Raman-based methods. J. Neuro Oncol. 151, 393–402.
Hoang-Xuan, Khe, et al., 2023. European Association of Neuro-Oncology (EANO) guidelines for treatment of primary central nervous system lymphoma (PCNSL). Neuro. Oncol. 25, 37–53.
Hollon, T.C., et al., 2020. Near real-time intraoperative brain tumor diagnosis using stimulated Raman histology and deep neural networks. Nat. Med. 26, 52–58.
Hollon, T., et al., 2023. Artificial-intelligence-based molecular classification of diffuse gliomas using rapid, label-free optical imaging. Nat Med 29, 828–832.
Kahraman, A., Dirilenoğlu, F., Güzeliş, İ., Çetinoğlu, K., 2024. Intraoperative pathologic diagnosis of central nervous system lymphomas: a comparison of frozen and permanent section diagnoses, and the significance of preoperative imaging. Ann. Diagn. Pathol. 69, 152246.
Klamminger, G.G., et al., 2021. Differentiation of primary CNS lymphoma and glioblastoma using Raman spectroscopy and machine learning algorithms. Free Neuropathol 2, 2–26.
Le, van D., R, K., Sj, D., Wr, G., 2021. Comparing object recognition in humans and deep convolutional neural networks-an eye tracking study. Front. Neurosci. 15.
Lukas, R.V., Stupp, R., Gondi, V., Raizer, J.J., 2018. Primary central nervous system lymphoma-PART 1: epidemiology, diagnosis, staging, and prognosis. Oncology (Williston Park) 32, 17–22.
Morell, A.A., et al., 2019. Diagnosis of primary central nervous system lymphoma: a systematic review of the utility of CSF screening and the role of early brain biopsy. Neurooncol Pract 6, 415–423.
Neidert, N., et al., 2022. Stimulated Raman histology in the neurosurgical workflow of a major European neurosurgical center — part A. Neurosurg. Rev. 45, 1731–1739.
Orringer, D.A., et al., 2017. Rapid intraoperative histology of unprocessed surgical specimens via fibre-laser-based stimulated Raman scattering microscopy. Nat. Biomed. Eng. 1, 1–13.
Pekmezci, M., et al., 2021. Detection of glioma infiltration at the tumor margin using quantitative stimulated Raman scattering histology. Sci. Rep. 11, 12162.
Reinecke, D., et al., 2024. Fast intraoperative detection of primary CNS lymphoma and differentiation from common CNS tumors using stimulated Raman histology and deep learning. https://doi.org/10.1101/2024.08.25.24312509.

Rubenstein, J.L., et al., 2013. Intensive chemotherapy and immunotherapy in patients with newly diagnosed primary CNS lymphoma: CALGB 50202 (Alliance 50202). J. Clin. Oncol. 31, 3061–3068.
Scheichel, F., et al., 2021. Influence of preoperative corticosteroid treatment on rate of diagnostic surgeries in primary central nervous system lymphoma: a multicenter retrospective study. BMC Cancer 21, 754.
Schorb, E., et al., 2016. High-dose chemotherapy and autologous stem cell transplant compared with conventional chemotherapy for consolidation in newly diagnosed primary CNS lymphoma–a randomized phase III trial (MATRix). BMC Cancer 16, 282.
Straehle, J., et al., 2022. Neuropathological interpretation of stimulated Raman histology images of brain and spine tumors: part B. Neurosurg. Rev. 45, 1721–1729.
Sugita, Y., et al., 2014. Intraoperative rapid diagnosis of primary central nervous system lymphomas: advantages and pitfalls. Neuropathology 34, 438–445.
Wang, X., et al., 2022. Transformer-based unsupervised contrastive learning for histopathological image classification. Med. Image Anal. 81, 102559.